Solvation structure of potassium bis(trifluoromethylsulfonyl)imide-glyme highly concentrated electrolytes and cycling on organic cathodes

Pieter Geysens,[a] Roy Heyns,[a] Robert Markowski,[b] Johannes Ingenmey,[c] Luc Van Meervelt,[a] Alexandru Vlad,[b] Barbara Kirchner,[c] Jan Fransaer[d] and Koen Binnemans[†]*

Electronic Supplementary Information (ESI)

Table S1. Specific Ionic Conductivity (σ), Dynamic Viscosity (η_{dyn}), Density (ρ), and Potassium Ion Concentration of G1–KTf_2N Electrolytes, Measured at 25 °C

Electrolyte G1:KTf_2N	σ at 25 °C (mS cm^{-1})	η_{dyn} at 25 °C (mPa s)	ρ at 25 °C (g cm^{-3})	K^+ concentration (mol dm^{-3})
50:1	2.3	0.5	0.90	0.19
40:1	3.1	0.6	0.91	0.23
30:1	4.7	0.6	0.93	0.31
20:1	7.2	0.7	0.96	0.45
15:1	8.9	0.8	0.98	0.59
10:1	12.1	1.1	1.03	0.85
8:1	12.6	1.3	1.07	1.02
6:1	13.3	2.1	1.12	1.30
5:1	13.6	2.8	1.16	1.50
4:1	11.7	4.1	1.21	1.77
3:1	9.7	8.4	1.28	2.17
2:1	4.6	24	1.38	2.77

Table S2. Specific Ionic Conductivity (σ), Dynamic Viscosity (η_{dyn}), Density (ρ), and Potassium Ion Concentration of G2–KTf_2N Electrolytes, Measured at 25 °C

Electrolyte G2:KTf_2N	σ at 25 °C (mS cm^{-1})	η_{dyn} at 25 °C (mPa s)	ρ at 25 °C (g cm^{-3})	K^+ concentration (mol dm^{-3})
50:1	1.4	1.2	0.96	0.14
40:1	1.8	1.2	0.97	0.17
30:1	2.7	1.3	0.98	0.23
20:1	4.0	1.5	1.00	0.33
15:1	5.1	1.7	1.02	0.44
10:1	6.5	2.3	1.06	0.64
8:1	7.0	2.7	1.09	0.78
6:1	6.9	3.7	1.12	1.00
5:1	6.8	4.9	1.15	1.17
4:1	6.3	6.9	1.19	1.39
3:1	5.1	12	1.25	1.73
2:1	3.7	32	1.34	2.28

Table S3. Specific Ionic Conductivity (σ), Dynamic Viscosity (η_{dyn}), Density (ρ), and Potassium Ion Concentration of G3–KTf_2N Electrolytes, Measured at 25 °C

Electrolyte G3:KTf_2N	σ at 25 °C (mS cm^{-1})	η_{dyn} at 25 °C (mPa s)	ρ at 25 °C (g cm^{-3})	K^+ concentration (mol dm^{-3})
50:1	0.8	2.3	1.00	0.11
40:1	1.0	2.3	1.01	0.14
30:1	1.4	2.4	1.01	0.18
20:1	2.0	2.7	1.03	0.27
15:1	2.5	3.0	1.04	0.35
10:1	3.5	3.6	1.07	0.51
8:1	3.9	4.1	1.09	0.62
6:1	3.9	5.5	1.12	0.81
5:1	3.9	6.9	1.15	0.95
4:1	n.d.	n.d.	n.d.	n.d.
3:1	n.d.	n.d.	n.d.	n.d.
2:1	n.d.	n.d.	n.d.	n.d.

n.d. = not determined, crystals present in the electrolytes

Table S4. Specific Ionic Conductivity (σ), Dynamic Viscosity (η_{dyn}), Density (ρ), and Potassium Ion Concentration of G4–KTf_2N Electrolytes, Measured at 25 °C

Electrolyte G4:KTf_2N	σ at 25 °C (mS cm^{-1})	η_{dyn} at 25 °C (mPa s)	ρ at 25 °C (g cm^{-3})	K^+ concentration (mol dm^{-3})
50:1	0.4	3.8	1.02	0.09
40:1	0.5	3.9	1.03	0.11
30:1	0.6	4.0	1.03	0.15
20:1	1.0	4.5	1.05	0.22
15:1	1.3	4.7	1.06	0.29
10:1	1.7	5.5	1.08	0.43
8:1	1.9	6.5	1.10	0.52
6:1	2.2	8.2	1.12	0.68
5:1	2.4	9.2	1.14	0.80
4:1	2.3	13	1.17	0.97
3:1	2.0	21	1.22	1.23
2:1	1.2	54	1.29	1.68

Table S5. Crystallographic data of $[K(G3)_2][Tf_2N]$

Solvate complex	$[K(G3)_2][Tf_2N]$
Empirical formula	$C_{8.5}H_{18}F_{1.5}K_{0.5}N_{0.25}O_5S_{0.5}$
Formula weight	267.81
Temperature/K	100(2)
Crystal system	triclinic
Space group	P-1
a/Å	8.6966(4)
b/Å	8.7794(4)
c/Å	20.5773(10)
α/°	80.5648(14)
β/°	79.6470(14)
γ/°	88.3127(14)
Volume/Å^3	1524.61(12)
Z	4
ρ_{calc}g/cm^3	1.167
μ/mm^{-1}	0.159
F(000)	567.0
Crystal size/mm^3	0.44 × 0.43 × 0.4
Radiation	AgKα (λ = 0.56086)
2Θ range for data collection/°	3.756 to 47.34
Index ranges	$-12 \leq h \leq 12$, $-12 \leq k \leq 12$, $-29 \leq l \leq 29$
Reflections collected	82585
Independent reflections	9344 [R_{int} = 0.0549, R_{sigma} = 0.0417]
Data/restraints/parameters	9344/0/365
Goodness-of-fit on F^2	1.049
Final R indexes [I>=2σ (I)]	R_1 = 0.0657, wR_2 = 0.1974
Final R indexes [all data]	R_1 = 0.0679, wR_2 = 0.2003
Largest diff. peak/hole / e Å^{-3}	3.20/-0.59
CCDC Deposition Code	2488110

Table S6. System composition, equilibrated box length, and density for molecular dynamics simulations of various systems at 350 K.

System	Glyme	KTf_2N	Box length *a* (Å)	ρ_{calc} at 350 K (g cm^{-3})
G1-KTf_2N 2:1	512	256	54.36	1.32
G1-KTf_2N 3:1	192	576	53.75	1.21
G1-KTf_2N 4:1	154	616	53.49	1.14
G2-KTf_2N 2:1	512	256	57.85	1.29
G2-KTf_2N 3:1	192	576	57.72	1.20
G2-KTf_2N 4:1	154	616	57.75	1.14
G3-KTf_2N 2:1	512	256	61.10	1.26
G3-KTf_2N 3:1	192	576	61.31	1.18
G3-KTf_2N 4:1	154	616	61.59	1.13
G4-KTf_2N 2:1	512	256	64.00	1.24
G4-KTf_2N 3:1	192	576	64.61	1.17
G4-KTf_2N 4:1	154	616	65.05	1.12

Table S7. Populations in % of K^+ cations coordinated by 0 to 6 Tf_2N^- anions in G1−KTf_2N 2:1 to 4:1.

# Tf_2N^-	2:1	3:1	4:1
0	0.41	1.26	1.98
1	10.51	17.99	26.81
2	40.26	53.17	51.58
3	37.44	24.65	18.44
4	10.49	2.91	1.19
5	0.87	0.03	0.01
6	0.01	0.00	0.00

Table S8. Populations in % of K^+ cations coordinated by 0 to 6 Tf_2N^- anions in G2–KTf_2N 2:1 to 4:1.

# Tf_2N^-	2:1	3:1	4:1
0	5.04	12.20	18.79
1	34.63	46.91	52.75
2	44.62	34.93	26.31
3	14.82	5.66	2.13
4	0.89	0.31	0.01
5	0.00	0.00	0.00
6	0.00	0.00	0.00

Table S9. Populations in % of K^+ cations coordinated by 0 to 6 Tf_2N^- anions in G3–KTf_2N 2:1 to 4:1.

# Tf_2N^-	2:1	3:1	4:1
0	37.94	51.09	53.84
1	30.40	36.48	38.45
2	27.90	12.07	7.42
3	3.76	0.36	0.29
4	0.00	0.00	0.00
5	0.00	0.00	0.00
6	0.00	0.00	0.00

Table S10. Populations in % of K^+ cations coordinated by 0 to 6 Tf_2N^- anions in G4–KTf_2N 2:1 to 4:1.

# Tf_2N^-	2:1	3:1	4:1
0	44.26	63.00	72.30
1	19.14	17.02	15.00
2	30.55	19.73	12.64
3	3.33	0.24	0.06
4	2.71	0.00	0.00
5	0.00	0.00	0.00
6	0.00	0.00	0.00

Table S11. Populations in % of Tf_2N^- anions coordinated by 0 to 6 K^+ cations in G1–KTf_2N 2:1 to 4:1.

# K^+	2:1	3:1	4:1
0	0.19	0.90	1.69
1	8.10	20.25	28.03
2	36.93	47.27	49.12
3	50.78	31.04	20.85
4	3.97	0.53	0.31
5	0.03	0.00	0.00
6	0.00	0.00	0.00

Table S12. Populations in % of Tf_2N^- anions coordinated by 0 to 6 K^+ cations in G2–KTf_2N 2:1 to 4:1.

# K^+	2:1	3:1	4:1
0	5.01	11.85	19.08
1	35.58	48.49	53.52
2	42.18	32.54	23.91
3	16.98	7.08	3.50
4	0.25	0.04	0.00
5	0.00	0.00	0.00
6	0.00	0.00	0.00

Table S13. Populations in % of Tf_2N^- anions coordinated by 0 to 6 K^+ cations in G3–KTf_2N 2:1 to 4:1.

# K^+	2:1	3:1	4:1
0	26.98	47.40	52.75
1	52.31	44.14	40.59
2	16.97	7.84	6.40
3	3.74	0.63	0.25
4	0.00	0.00	0.00
5	0.00	0.00	0.00
6	0.00	0.00	0.00

Table S14. Populations in % of Tf_2N^- anions coordinated by 0 to 6 K^+ cations in G4–KTf_2N 2:1 to 4:1.

# K^+	2:1	3:1	4:1
0	31.20	51.76	67.53
1	42.37	39.69	29.22
2	20.73	8.10	3.25
3	5.52	0.44	0.00
4	0.18	0.00	0.00
5	0.00	0.00	0.00
6	0.00	0.00	0.00

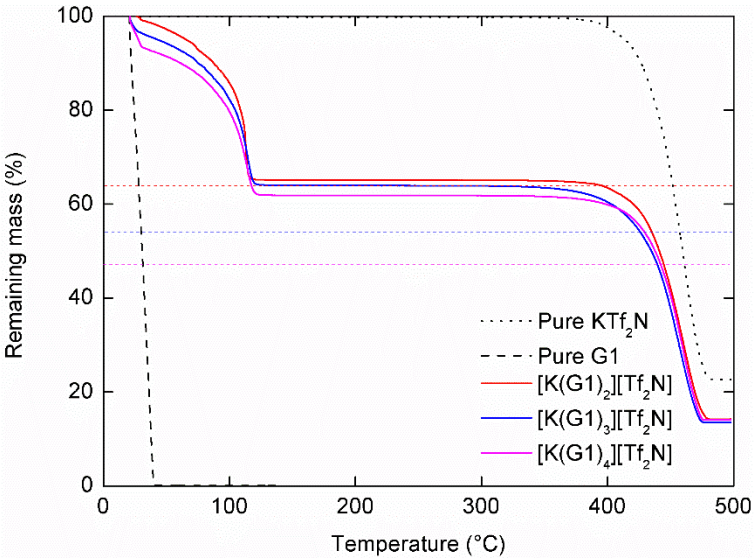

Figure S1. Dynamic TGA curves of $[K(G1)_2][Tf_2N]$, $[K(G1)_3][Tf_2N]$ and $[K(G1)_4][Tf_2N]$ (full lines), pure G1 (dashed line) and pure KTf_2N (dotted line), recorded at 5 °C min^{-1}. The horizontal dotted lines represent the theoretical remaining mass for each solvate complex after loss of all ligands.

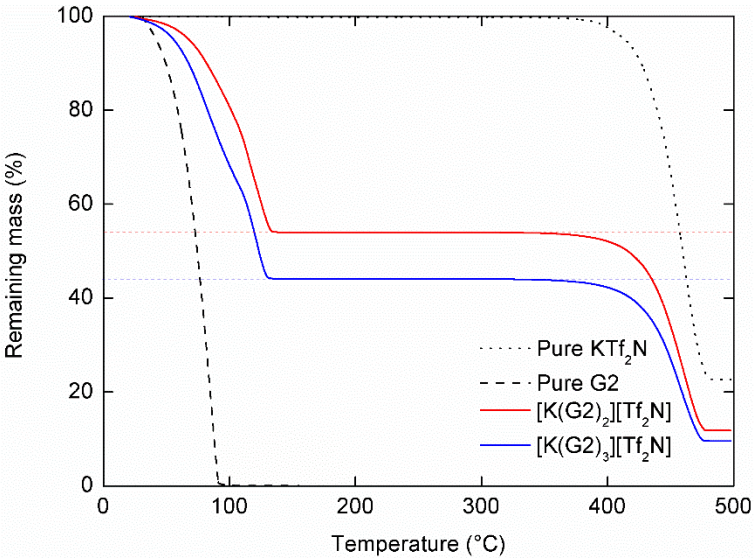

Figure S2. Dynamic TGA curves of $[K(G2)_2][Tf_2N]$ and $[K(G2)_3][Tf_2N]$ (full lines), pure G2 (dashed line) and pure KTf_2N (dotted line), recorded at 5 °C min^{-1}. The horizontal dotted lines represent the theoretical remaining mass for each solvate complex after loss of all ligands.

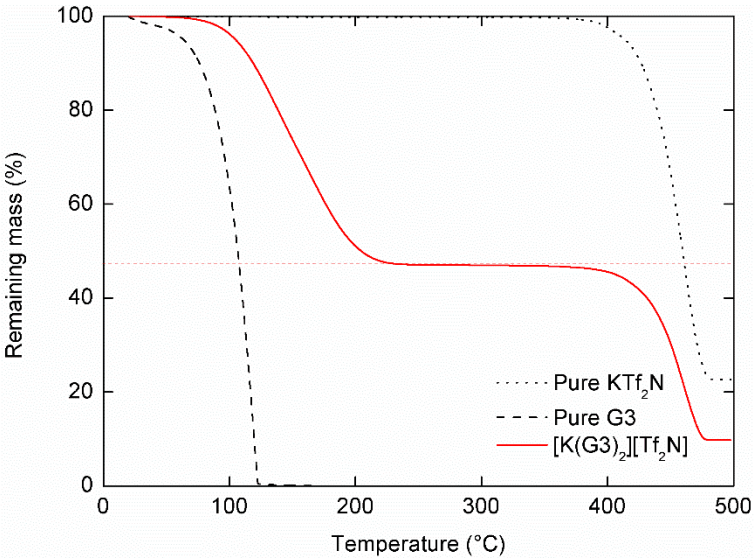

Figure S3. Dynamic TGA curves of $[K(G3)_2][Tf_2N]$ (full line), pure G3 (dashed line) and pure KTf_2N (dotted line), recorded at 5 °C min^{-1}. The horizontal dotted lines represent the theoretical remaining mass for the solvate complex after loss of all ligands.

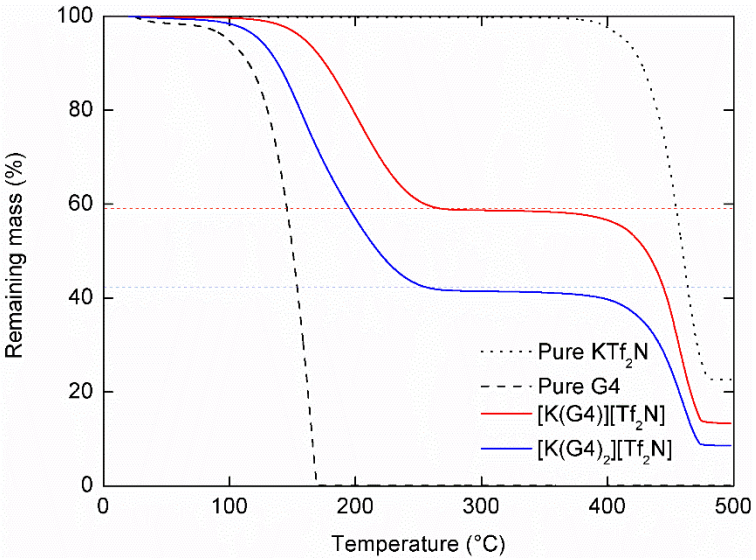

Figure S4. Dynamic TGA curves of [K(G4)][Tf_2N] and [$K(G4)_2$][Tf_2N] (full lines), pure G4 (dashed line) and pure KTf_2N (dotted line), recorded at 5 °C min^{-1}. The horizontal dotted lines represent the theoretical remaining mass for each solvate complex after loss of all ligands.

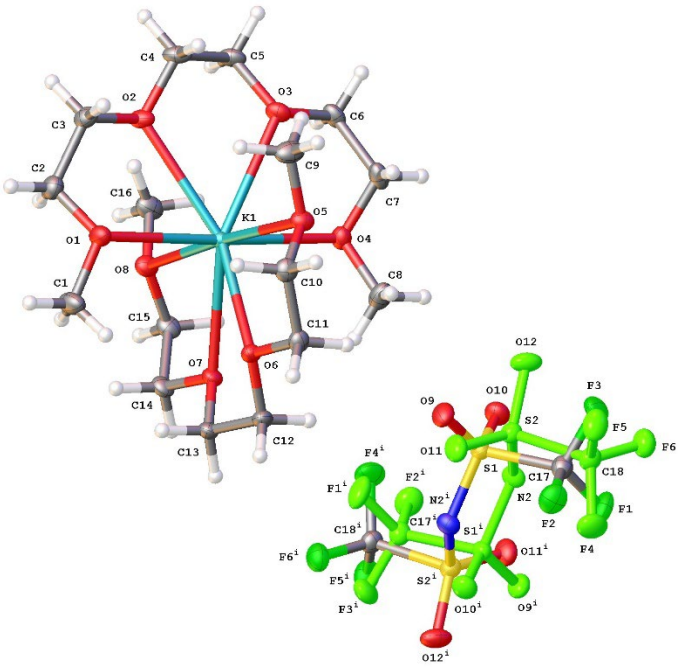

Figure S5. Close-up view of the solvate structure of $[K(G3)_2][Tf_2N]$. Thermal ellipsoids are shown at the 30% probability level. The labels of hydrogen atoms are omitted for clarity. Disorder on the Tf_2N^- anion is shown. Cyan, K; red, O; grey, C; white, H; yellow, S; green, F; blue, N. Symmetry code: (i) -x, 1 - y, 2 - z.

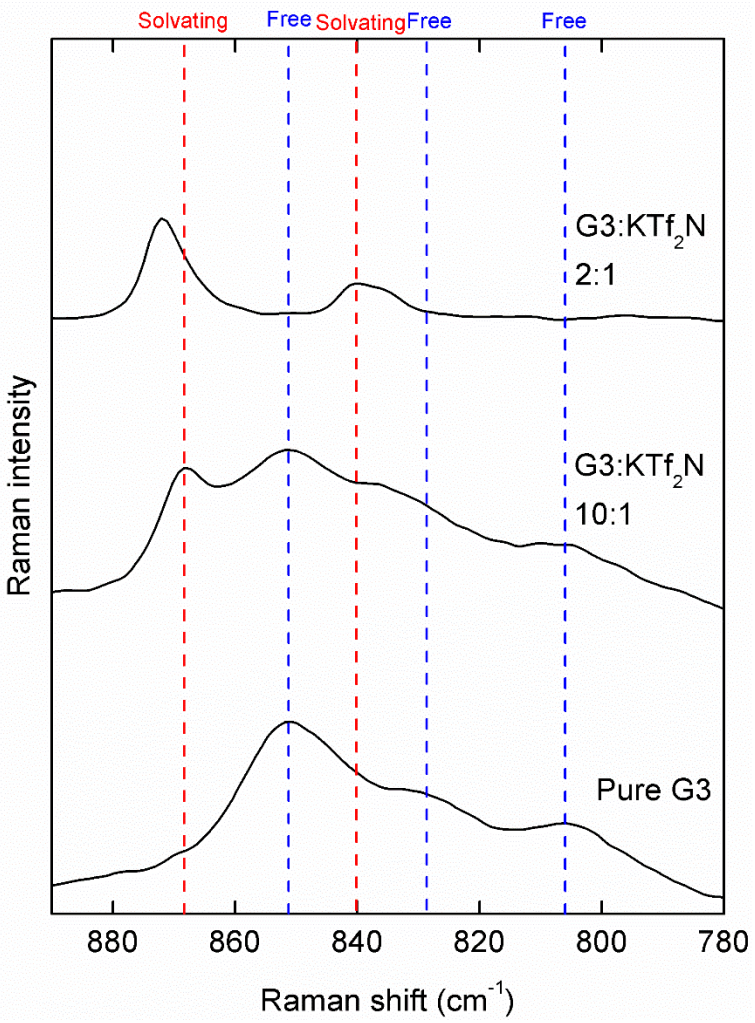

Figure S6. Concentration dependance of the Raman spectra in the range 780–890 cm^{-1} for G3–KTf_2N mixtures.

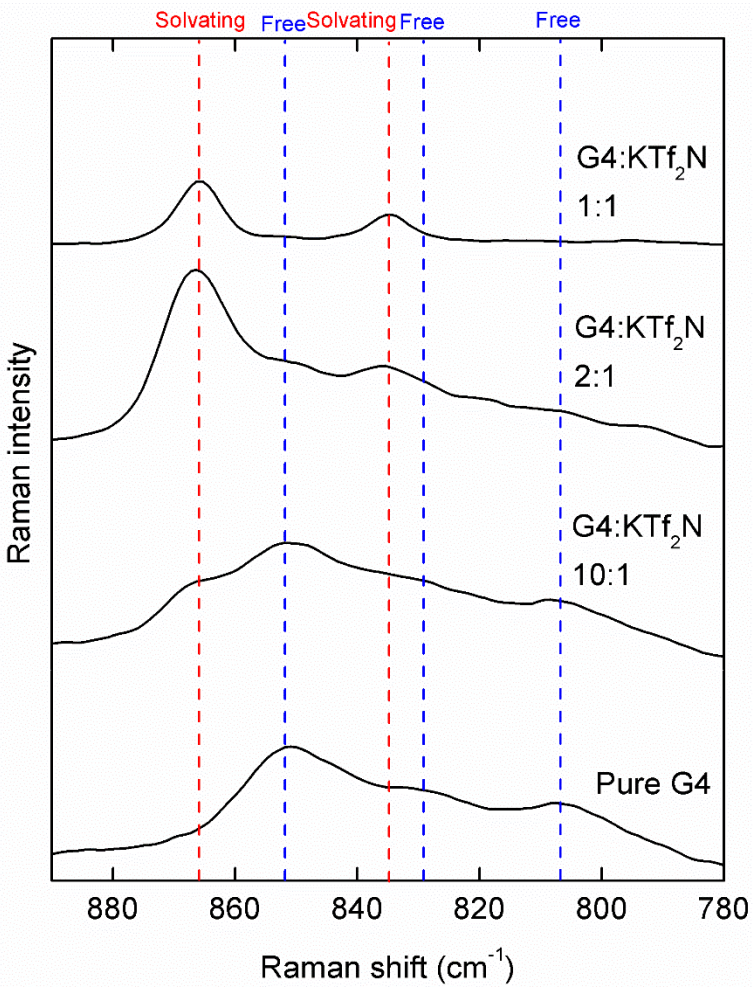

Figure S7. Concentration dependance of the Raman spectra in the range 780–890 cm^{-1} for G4–KTf_2N mixtures.

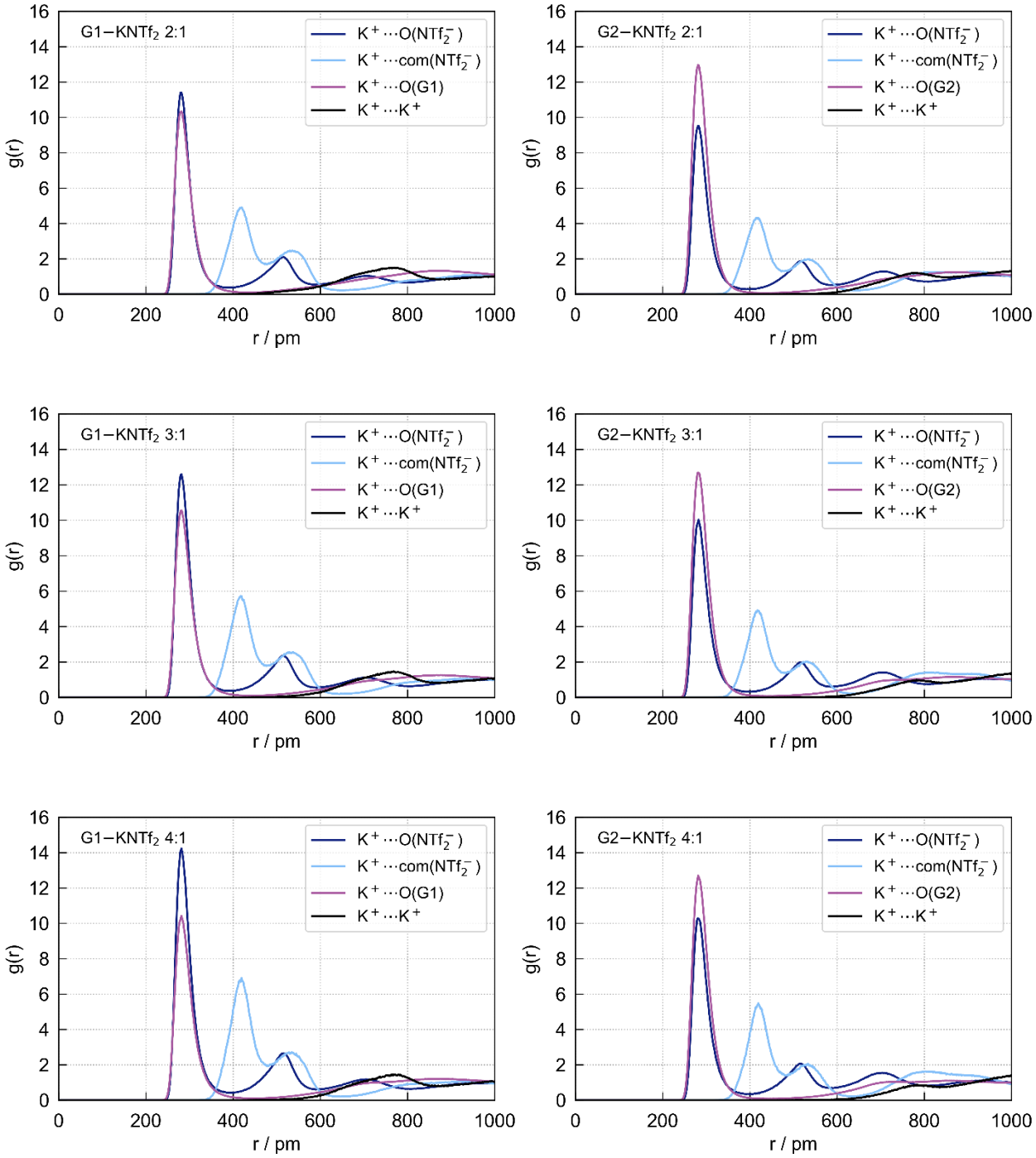

Figure S8. Radial distribution functions of the K^+ cation interacting with different moieties in G1–KTf_2N (left) and G2–KTf_2N (right) mixtures of composition 2:1 (top), 3:1 (center), and 4:1 (bottom).

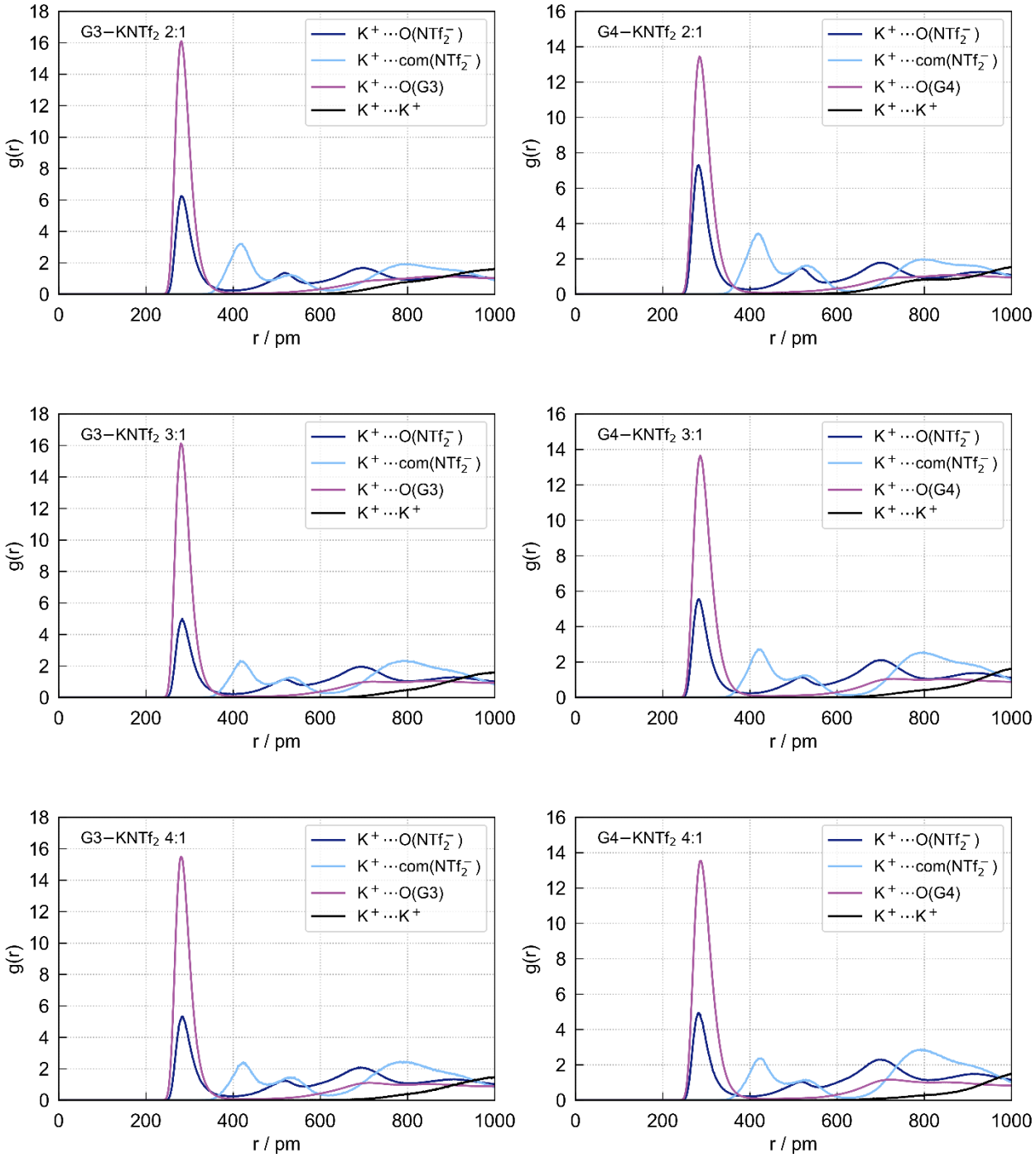

Figure S9. Radial distribution functions of the K^+ cation interacting with different moieties in G3–KTf_2N (left) and G4–KTf_2N (right) mixtures of composition 2:1 (top), 3:1 (center), and 4:1 (bottom).

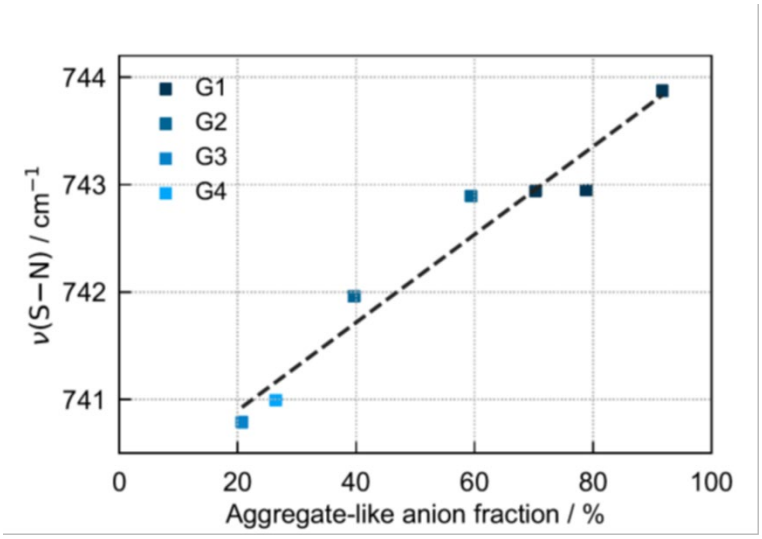

Figure S10. Correlation of the Raman ν(SN) peak position with the fraction of Tf_2N^- anions bound in AGG structures, as obtained from MD. Each point corresponds to a specific glyme and salt concentration. The dashed line is a linear fit meant to guide the eye.

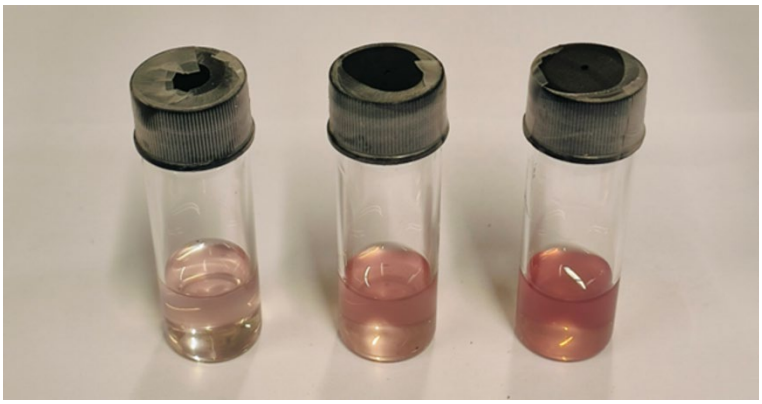

Figure S11. Solubility test of pure K2–Co–PTtSA in, from left to right, $[K(G2)_2][Tf_2N]$, $[K(G1)_2][Tf_2N]$, and the standard 1 mol L^{-1} KPF_6 in EC:PC electrolyte.